THE ASTROPHYSICAL JOURNAL, 331:784–793, 1988 August 15

LIMITS ON ROTATION-INDUCED CHARACTERISTICS OF RADIATION FROM STABLE RAPIDLY ROTATING NEUTRON STARS

B. DATTA[1] AND R. C. KAPOOR
Indian Institute of Astrophysics
Received 1987 July 7; accepted 1988 February 9

ABSTRACT

Results are presented of a study of frequency shifts in radiation from the surface of rapidly rotating neutron stars and rotation-induced spectral line broadening as a function of their mass. We find that, despite large rotation rates, the gravitational effects dominate over the Doppler contribution to the frequency shifts over the allowed mass range of a stable rotating neutron star. Astrophysical implications of effect of large rotation on spectral line characteristics are also discussed.

Subject headings: stars: neutron — stars: rotation

I. INTRODUCTION

Observational estimates of neutron star masses are made using binary pulsar data (Joss and Rappaport 1984, and references therein). On the other hand, interpretation of gamma-ray lines from gamma-ray burst sources in the energy band (0.4–0.46) MeV as redshifted e^+e^- annihilation line from surfaces of neutron stars provides an estimate for the mass-to-radius ratio (M/R) of the star. These constitute the conventional approach in estimating neutron star structure parameters and hence serve as possible constraints on the validity of equation of state of high density matter. With the discovery of millisecond pulsars and the possible existence of rapidly rotating neutron stars in X-ray sources (Imamura, Steiman-Cameron, and Middleditch 1987), it is reasonable to ask if such objects are sources of gamma-ray line emission, and, if so, what are the new effects that a large rotation rate will have on the spectral characteristics of the radiation. Kapoor and Datta (1984) have recently demonstrated that a large rotation rate will substantially modify the spectral characteristics of gamma-ray line emission from rotating neutron stars. In particular, it was shown that the effect of a large rotation rate will be to produce a broadened spectral line with a profile that is highly asymmetrical, producing the appearance of a "blueshifted line" rather than a mere broadened one. In view of this, it will be incorrect to extend the usual interpretation of redshifted line emission to determine M/R for the case of rapidly rotating neutron stars. The study in Kapoor and Datta (1984) was illustrated for the 1.56 ms pulsar PSR 1937+214, assuming its mass to be 1.4 $M_\odot$. In this paper we present a detailed study of frequency shifts in radiation from the surface of rapidly rotating neutron stars as a function of mass, using a representative set of equations of state for high-density matter.

For a pulsar, millisecond periods suggest that the object is close to the secular rotational instability limit (Ray and Datta 1984). Thus, we use here neutron star models rotating at the secular instability point. The angular speed corresponding to the secular instability point increases with the mass of the neutron star; therefore, a relevant question is how the contribution of the Doppler effect to frequency shifts varies over the allowed mass range of the stable neutron star. We address this question in detail here and also point out its astrophysical implications.

[1] Biren Roy Trust Fellow of the Indian National Science Academy.

II. ROTATING NEUTRON STAR AND FREQUENCY SHIFT

The Kerr solution, which provides the full rotational analog to the spherically symmetric spacetime, does not have a corresponding appropriate interior solution amenable to straightforward theoretical study and a quantitative estimate of structural parameters. It is, however, adequate to use structural parameters calculated from a formalism specific to a rotationally perturbed interior spherical metric with a corresponding exterior metric matching at the surface. Such a formalism was first given by Hartle (1967), and it can be used to provide a wide variety of useful information regarding the structure and radiation characteristics of fast pulsars (Datta and Ray 1983; Ray and Datta 1984; Kapoor and Datta 1984, 1985, 1986; Datta and Kapoor 1985). The metric in this formalism has the following form ($c = G = 1$)

$$ds^2 = e^{2\nu}dt^2 - e^{2\psi}(d\phi - \omega\, dt)^2 - e^{2\mu}d\theta^2 - e^{2\lambda}dr^2 + O(\Omega^3/\Omega_c^3)\,. \quad (1)$$

Here Ω is the angular velocity of the neutron star as measured by a remote observer, $\Omega_c = (M/R^3)^{1/2}$, and M and R are the mass and radius of the nonrotating configuration. The metric components corresponding to an exterior spacetime ($r \geq R'$) are

$$e^{2\nu} = e^{-2\lambda} = \left(1 - \frac{2M'}{r} + \frac{2J^2}{r^4}\right),$$
$$e^{2\psi} = r^2 \sin^2\theta\,, \quad (2)$$
$$e^{2\mu} = r^2\,.$$

Here $M' = M + \delta M$ and $R' = R + \delta R$, where δM and δR are the rotationally induced spherical deformation terms in the mass and radius of the neutron star, respectively, and J is its angular momentum. The quantity

$$\omega = 2J/r^3 \quad (3)$$

is the angular velocity of cumulative dragging of inertial frames. The above geometry is valid for strong gravitational fields, but, in the limit of uniform rotation with a rate that is slow compared to Ω_c, which is the critical angular velocity for centrifugal breakup. A homogeneous neutron star which rotates at the secular instability limit (Tassoul 1978)

$$\Omega_s = 0.52\Omega_c\,, \quad (4)$$

relevant for fast pulsars, is within this bound. Structural calculations for neutron stars for realistic equations of state with $\Omega = \Omega_s$ were made by Ray and Datta (1984) using the above formalism. The condition of rotational instability, equation (4), was applied by Datta and Ray (1983) to the 1.56 ms pulsar PSR 1937+214 to estimate a lower bound on the mass and moment of inertia for fast pulsars and upper bound on the radius ($M'_{\min}$, $I'_{\min}$, $R'_{\max}$). The condition of hydrostatic equilibrium and stability with respect to radial perturbations provides another set of limits: ($M'_{\max}$, $I'_{\max}$, $R'_{\min}$). These limits depend on the equation of state. One thus has a range in the structural parameters of stable, rotating neutron stars which is specific to the equation of state used. Our calculations here refer to rotating neutron stars with $\Omega = \Omega_s$, and structural parameters spanning over this range.

When rotation is absent, the redshift factor of a star with mass M and radius R is derived using Schwarzschild metric, and it has the following form:

$$1 + z_s \equiv Z_s = (1 - 2M/R)^{-1/2} . \tag{5}$$

Lindblom (1984) has given extreme values of neutron star redshifts using Schwarzschild formalism, and such a general condition as the velocity of sound in dense matter is positive definite and obeys causality limit.

To derive the expression for the redshift factor corresponding to the metric in equation (1), we use the geometrical optics approximation that photons are zero rest mass particles propagating along null trajectories. The general expression for frequency shift is as follows (for the detailed derivation, see Kapoor and Datta 1984):

$$1 + z_R \equiv Z_R = \frac{1 + \Omega q}{e^{\nu}(1 - V_s^2)^{1/2}} . \tag{6}$$

In equation (6), V_s is the tangential velocity of an emitter at $r = r_e$ and $\theta = \theta_s$ as seen by a locally nonrotating observer:

$$V_s = e^{\psi - \nu}(\Omega - \omega) . \tag{7}$$

The angle θ_s, the polar angle of emission of the photon, can be taken to be the angle of inclination of the neutron star since we use only a rotationally perturbed form of a spherical metric (Kapoor and Datta 1984). Thus $\theta_s = 0$ means that we look along the pole of the rotating neutron star, while $\theta_s = \pi/2$ refers to equatorial emission. The quantity q in equation (6) is the impact parameter of the photon which is emitted at angle δ with respect to the radial direction such that it increases in the direction opposite to that of rotation of the star:

$$q = \frac{e^{\psi - \nu}(V_s + \sin \delta)}{1 + e^{\psi - \nu}(\omega V_s + \Omega \sin \delta)} . \tag{8}$$

The surface redshift of a neutron star $(Z_R)_{r_e = R'}$ corresponds to $q = 0$. It may be noted that $q = 0$ does not imply radial emission unless rotational terms are suppressed. Thus the $Z_R(\delta = 0)$ values will differ from $Z_R(q = 0)$ values as a result of inertial frame drag effect. Moreover, presence of a term with V_s implies a second-order dependence of redshift on polar angle of emission, which can be identified as the Doppler contribution from a "$V \sin i$" kind of a term.

The injection energy of a unit mass particle lowered onto the neutron star from infinity is given as

$$I_e = (e^{2\nu})_{\theta_s = 0} , \tag{9}$$

which can be related to the polar redshift of the rotating neutron star through

$$Z_R(\theta_s = 0) = e^{-\nu} . \tag{10}$$

Emission of gamma-ray lines from the surface of rotating neutron stars is an interesting possibility (Kapoor and Datta 1984). Rotation broadens spectral line and the resulting width of a gamma-ray line can be written as

$$W = E_{\rm em} \frac{\Omega e^{\nu}(1 - V_s^2)^{1/2}[q(\delta = \pi/2) - q(\delta = -\pi/2)]}{[1 + \Omega q(\delta = \pi/2)][1 = \Omega q(\delta = -\pi/2]} , \tag{11}$$

where $E_{\rm em}$ is the emission energy.

Application of the requirement of conservation of particles in phase space to electromagnetic radiation implies that blue and red ends of the Doppler-broadened gamma-ray lines will suffer Doppler boosting and diminution, respectively. The ratio of intensities at two ends of the line will be

$$r_{\rm IN} = \frac{I_{\rm blue}}{I_{\rm red}} = \left[\frac{Z_R(\delta = -\pi/2)}{Z_R(\delta = \pi/2)}\right]^{-3} . \tag{12}$$

III. RESULTS AND DISCUSSION

In this paper we choose the following five equations of state (EOS) based on a representative choice of neutron and nuclear matter interactions:

1) Reid-Pandharipande (RP);
2) Friedman-Pandharipande (FP);
3) Canuto-Datta-Kalman (CDK);
4) Bethe-Johnson (BJ) Model I;
5) Tensor Interaction (TI).

The details regarding the composite equation of state and the corresponding rotating neutron star models are given in Ray and Datta (1984). Table 1 lists neutron star parameters such as

TABLE 1

STRUCTURAL PARAMETERS FOR REDSHIFT CALCULATIONS

EOS	M' ($M_\odot$)	J' (10^{48} cgs)	R' (10^6 cm)	Ω_s (10^3 rad s^{-1})	R'/M'
RP	0.700	1.613	1.170	4.033	11.347
	0.899	2.680	1.117	4.890	8.435
	1.294	5.304	1.049	6.360	5.504
	1.521	7.363	0.994	7.430	4.437
	1.694	9.523	0.910	8.900	3.647
FP	0.760	2.017	1.200	4.033	10.720
	1.197	4.674	1.150	5.330	6.522
	1.592	8.150	1.083	6.680	4.618
	1.924	12.490	1.008	8.110	3.557
	2.085	15.650	0.929	9.483	3.025
CDK	0.790	1.896	1.200	4.033	10.312
	1.137	4.300	1.182	5.000	7.058
	1.459	6.675	1.176	5.477	5.472
	1.492	7.386	1.172	5.770	5.333
	1.867	11.610	1.110	6.960	4.036
BJ	1.200	4.437	1.390	4.033	7.864
	1.218	4.708	1.382	4.130	7.703
	1.419	6.236	1.317	4.760	6.301
	1.895	11.340	1.116	6.960	3.998
	1.965	12.570	1.014	8.160	3.503
TI	1.720	6.050	1.560	4.033	6.158
	1.756	9.693	1.520	4.270	5.876
	1.800	10.570	1.450	4.472	5.469
	1.850	10.620	1.350	5.309	4.954
	1.873	10.400	1.261	5.810	4.571

NOTE.—Entries are taken from Ray and Datta 1984. For M', J, and Ω_s, entries in the first (last) row for each EOS correspond to their minimum (maximum) values, and conversely for R and R'.

TABLE 2

LIMITING VALUES OF SURFACE REDSHIFT FOR SCHWARZSCHILD AND ROTATIONAL CASES

	SCHWARZSCHILD						ROTATIONAL							
EOS	M_{min} ($M_\odot$)	R_{max} (10^6 cm)	Z_s	M_{max} ($M_\odot$)	R_{min} (10^6 cm)	Z_s	M'_{min} ($M_\odot$)	R'_{max} (10^6 cm)	θ_s	Z_R	M'_{max} ($M_\odot$)	R'_{min} (10^6 cm)	θ_s	Z_R
RP	0.65	1.124	1.098	1.60	0.897	1.452	0.70	1.17	0	1.145	1.694	0.910	0	1.486
									$\pi/2$	1.168			$\pi/2$	1.568
FP	0.70	1.152	1.104	1.98	0.924	1.647	0.76	1.20	0	1.109	2.085	0.929	0	1.711
									$\pi/2$	1.126			$\pi/2$	1.827
CDK	0.73	1.154	1.108	1.74	1.088	1.375	0.79	1.20	0	1.114	1.867	1.110	0	1.408
									$\pi/2$	1.131			$\pi/2$	1.475
BJ	1.11	1.342	1.151	1.87	1.002	1.490	1.20	1.39	0	1.158	1.965	1.014	0	1.523
									$\pi/2$	1.183			$\pi/2$	1.613
TI	1.59	1.511	1.204	1.77	1.232	1.317	1.72	1.56	0	1.218	1.873	1.261	0	1.334
									$\pi/2$	1.255			$\pi/2$	1.391

M', R', J, and $\Omega_s(M')$ for the various equations of state covering the entire range provided by the instability criteria (see § II). The radiation is assumed to originate at a radial location $r_e = R'$. The results for the red-shift factor are presented in the Table 2 and Figures 1–11.

Table 2 lists the range in extreme values of surface redshifts, corresponding to the limiting values of the mass for nonrotating (Schwarzschild) configurations as well as of the corresponding secularly rotating configurations. The largest neutron star mass ($=2.085\ M_\odot$) occurs in the case of an FP model which also accommodates largest amount of rotation ($\Omega_s = 9.483 \times 10^3$ rad s^{-1} or a period $= 0.66$ ms), a rate more than twice the rotation rate of the 1.56 ms pulsar. This configuration has the largest surface redshift factor of 1.71 (polar) and 1.83 (equatorial). The values in Table 2 for nonrotating configurations have a range narrower than that given by Lindblom (1984).

In Figures 1 and 2, mass versus surface redshifts are plotted for Schwarzschild, and the corresponding secularly rotating configurations for all the five equations of state, covering the entire stable mass range. These figures offer an interesting comparison among themselves. In the rotational case, the curves in fact are *bands* as a result of θ_s dependence of the redshift factor $1 + z_R = Z_R$. The band structure is composed of curves of variation of M' with $Z_R(\theta_s)$ where the band boundaries correspond to polar and equatorial cases ($\theta_s = 0$ and $\theta_s = \pi/2$, respectively) for $M' =$ constant lines, the equatorial case values being to the right of the polar redshifts values. The widest range in mass and the surface redshift values is allowed by the FP equation of state. In contrast, configurations corresponding to the TI equation of state have the narrowest range in mass and the surface redshift.

Figures 3–7 illustrate contribution of the Doppler effect to gravitational redshift. This is shown by plotting values of fre-

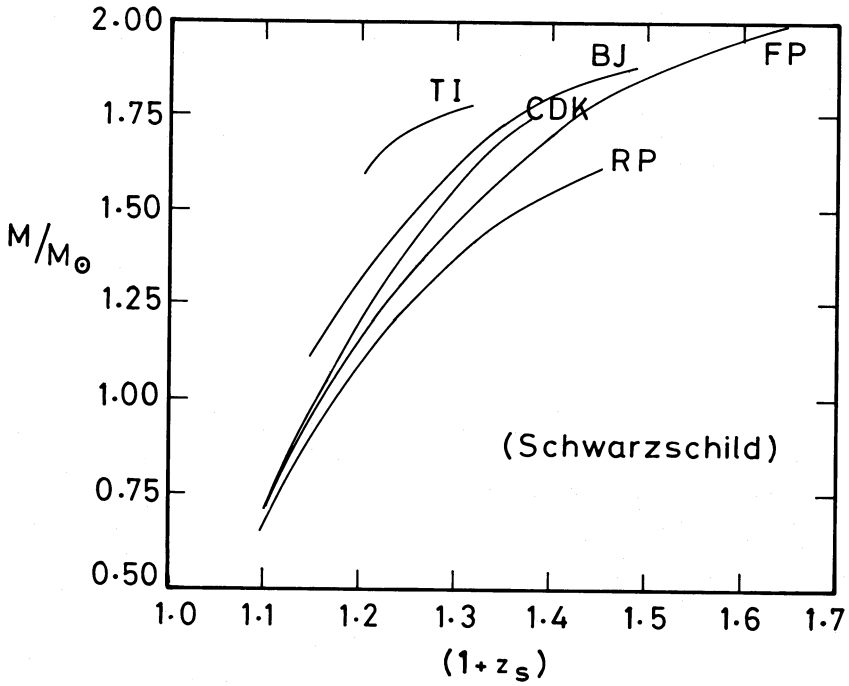

FIG. 1.—Variation of surface redshift as a function of nonrotating mass for the various EOS

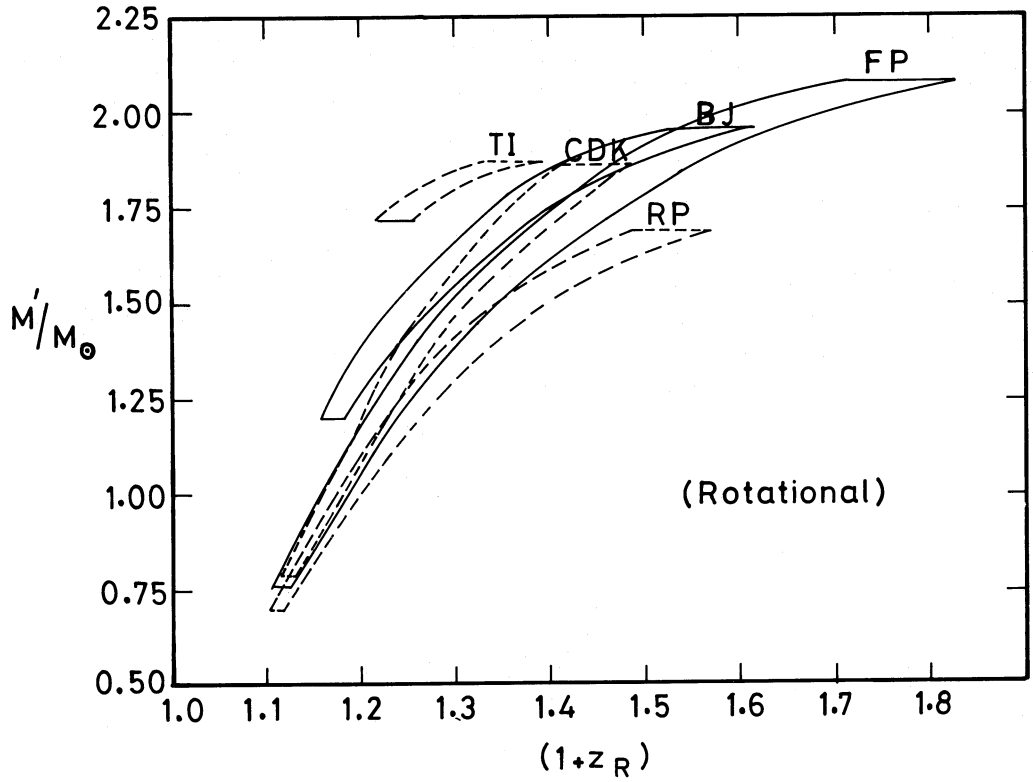

FIG. 2.—Variation of surface redshift of a rotating neutron star as a function of its mass. Intercepts of M' = constant lines with a band represent variation of redshift with respect to the polar inclination angle θ_s, the left arm of a band corresponds to polar redshift whereas the right arm to equatorial redshift (see text).

quency shift in radiation from the surface of the rotating neutron star in forward ($\delta = -\pi/2$) and backward ($\delta = \pi/2$) directions as a function of polar angle of emission such that

$$(Z_R)_{\min} = (1 + z_R)_{\delta = -\pi/2} ,$$
$$(Z_R)_{\max} = (1 + z_R)_{\delta = \pi/2} .$$

The ordinate of a curve corresponding to a configuration of mass M' on the vertical axis is actually its polar redshift. We find that in general the frequency shifts do not have a strong dependence on θ_s. Within the range in frequency shifts so provided, the additive and subtractive contribution of Doppler effect to gravitational redshift is noticeable in the various mass configurations for all the equations of state. It can be inferred from these figures that for a larger mass of the neutron star the gap between $(Z_R)_{\max}$ (Doppler plus gravitational) and $(Z_R)_{\min}$ values (gravitational minus Doppler) is wider for $\theta_s =$ constant, since a larger mass has a higher value of angular velocity, Ω_s, and this increases the magnitude of the Doppler contribution. This gap is the widest for $M' = 2.085\ M_\odot$ configuration of the FP equation of state. However, in the case of equatorial emission, while the range in $(Z_R)_{\max}$ values is the widest over the mass spectrum, that in the $(Z_R)_{\min}$ values for different masses is comparatively narrow, and $(Z_R)_{\min} \approx 1$. A switchover in the frequency shifts (from red to blue) is found to occur, and it generally happens for all masses and equations of state *as early as* $\theta_s \approx 0.2\pi$. Further, for a given equation of state, the higher the mass, the blueshifts occur at a larger polar inclination. Figure 8 is a plot similar to Figures 3–7 but corresponds to a 1.4 $M_\odot$ mass configuration with $\Omega = \Omega_s$.

The Doppler contribution to frequency shift is better understood by noting that the $V_s(\theta_s)$ values are approximately directly proportional to the mass of the rotating configuration where $V_s(\theta_s)$ for M' = constant is sinusoidal in θ_s. Figure 9 depicts the relationship between the mass of a rotating configuration and the tangential equatorial velocity of its rotation as measured by a locally nonrotating observer at $r_e = R'$. The maximum tangential velocity, with a value of $V_s\ (\theta_s = \pi/2) \approx 0.35$ occurs in the case of the 2.085 $M_\odot$ configuration of the FP equation of state. *Our calculations show that gravitational effects start prevailing over the Doppler contribution to the frequency shift as mass of the secular configuration is increased, for all the equations of state over a wide range of polar inclination angles.*

To calculate the effect of rotation on spectral line broadening, we choose the 511 keV e^+e^- annihilation line for the purpose of illustration. We further assume that the emission takes place from the surface and that the emission region is negligibly thin compared to the stellar radius, this to ensure that the broadening is purely Doppler with no effect arising from a gravitation potential well. The line widths (W) have a marked dependence on θ_s, being zero for $\theta_s = 0$ and have a maximum value in the equatorial plane (Figure 10). The widths have a fairly large magnitude for $\theta_s \gtrsim 0.2\pi$, and in the case of FP equation of state, would be as high as ~ 500 keV (for the 2.085 $M_\odot$ mass configuration). It may be commented here that a broadened spectral line will be asymmetrically placed with respect to the line center [since $q(+\delta) \neq q(-\delta)$] which itself is redshifted with respect to the rest wavelength of radiation. This is a consequence of the inertial frame drag effect.

Due to rotation, the $(-\delta)$ photons are Doppler boosted, whereas $(+\delta)$ photons are Doppler diminished so that there will result an asymmetry in the line profile. Leaving aside the

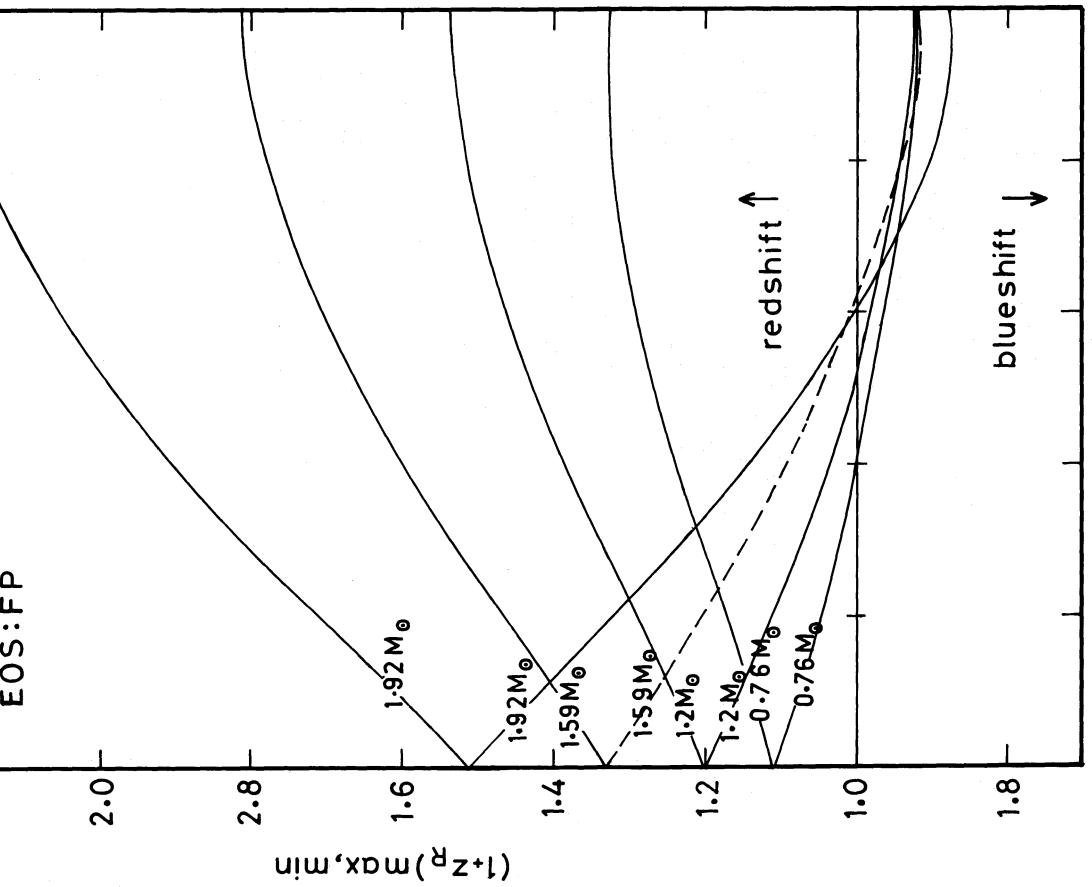

FIG. 4

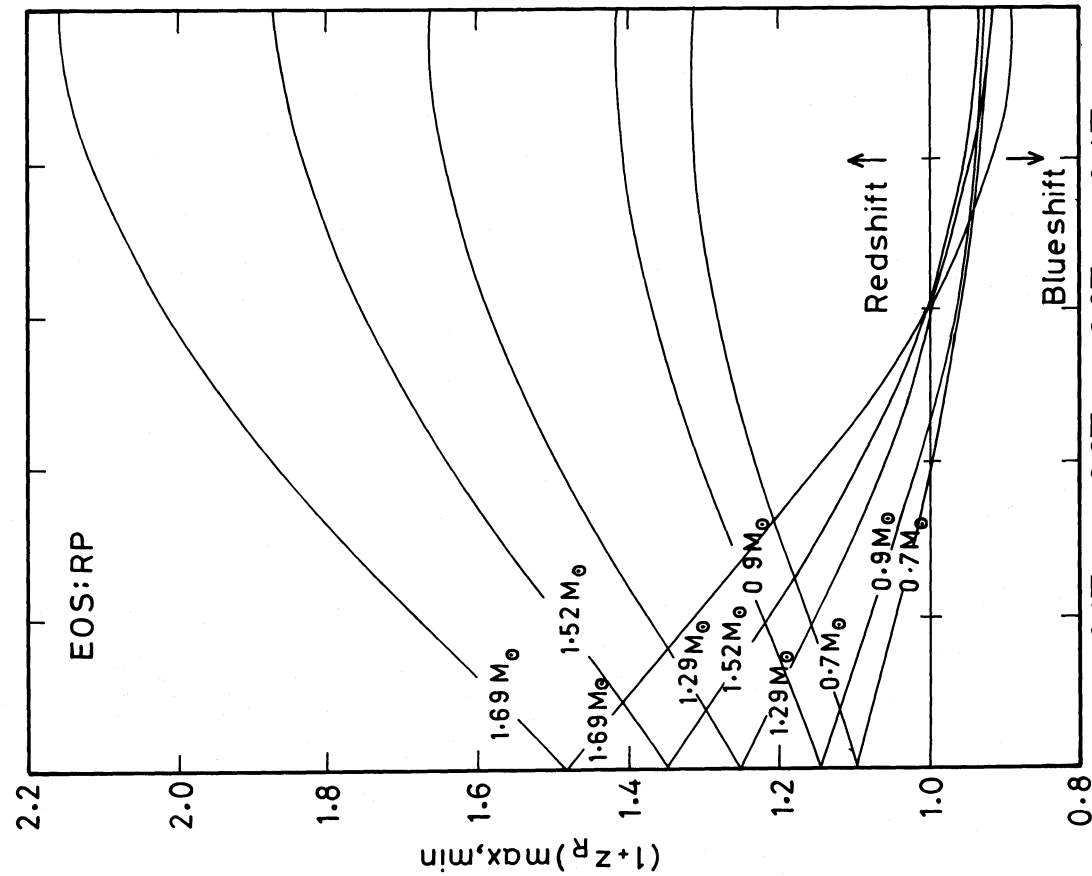

FIG. 3

FIG. 3.—Variation of frequency shift of forward $(Z_R)_{min}$ and backward $(Z_R)_{max}$ as a function of polar angle of emission for different masses. EOS model: RP.
FIG. 4.—Same as Fig. 3, but for EOS model: FP

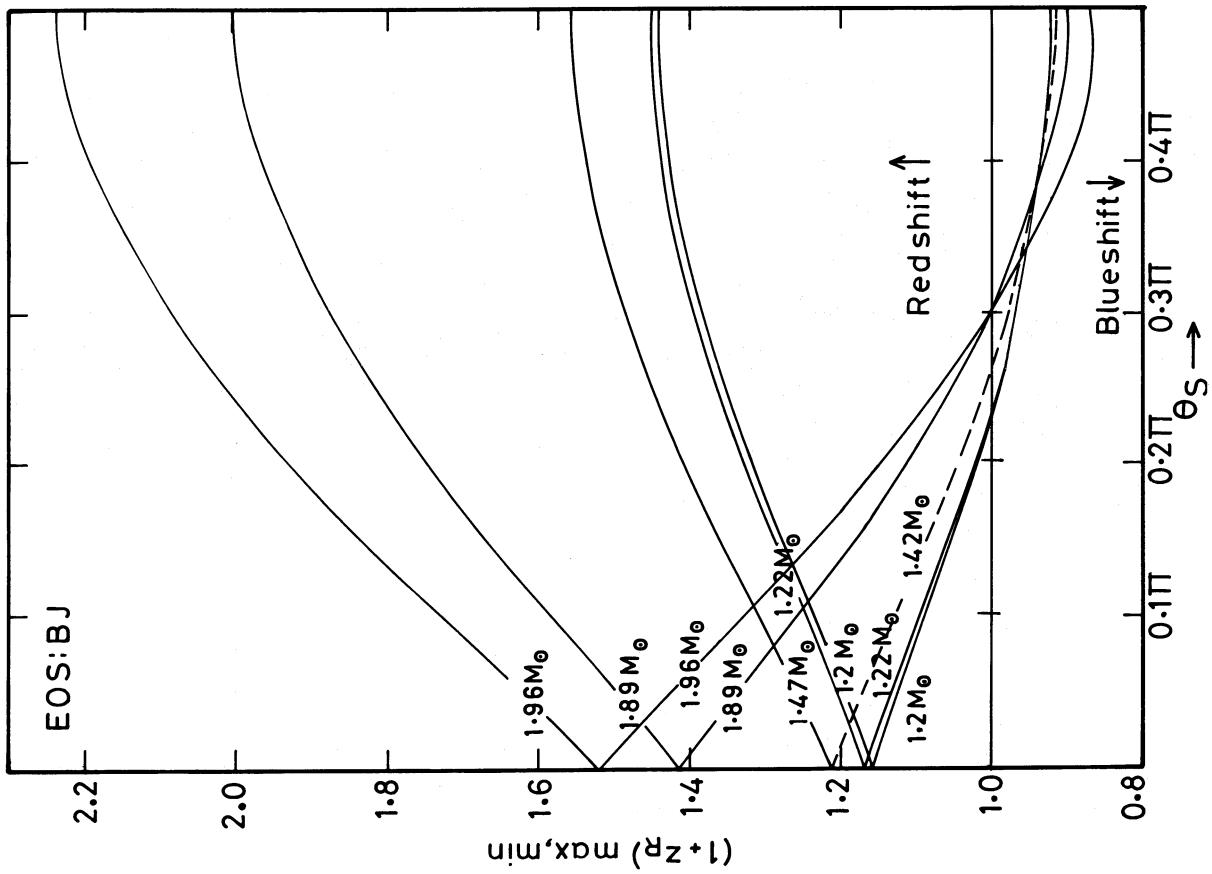

FIG. 6.—Same as Fig. 3, but for EOS model: BJ

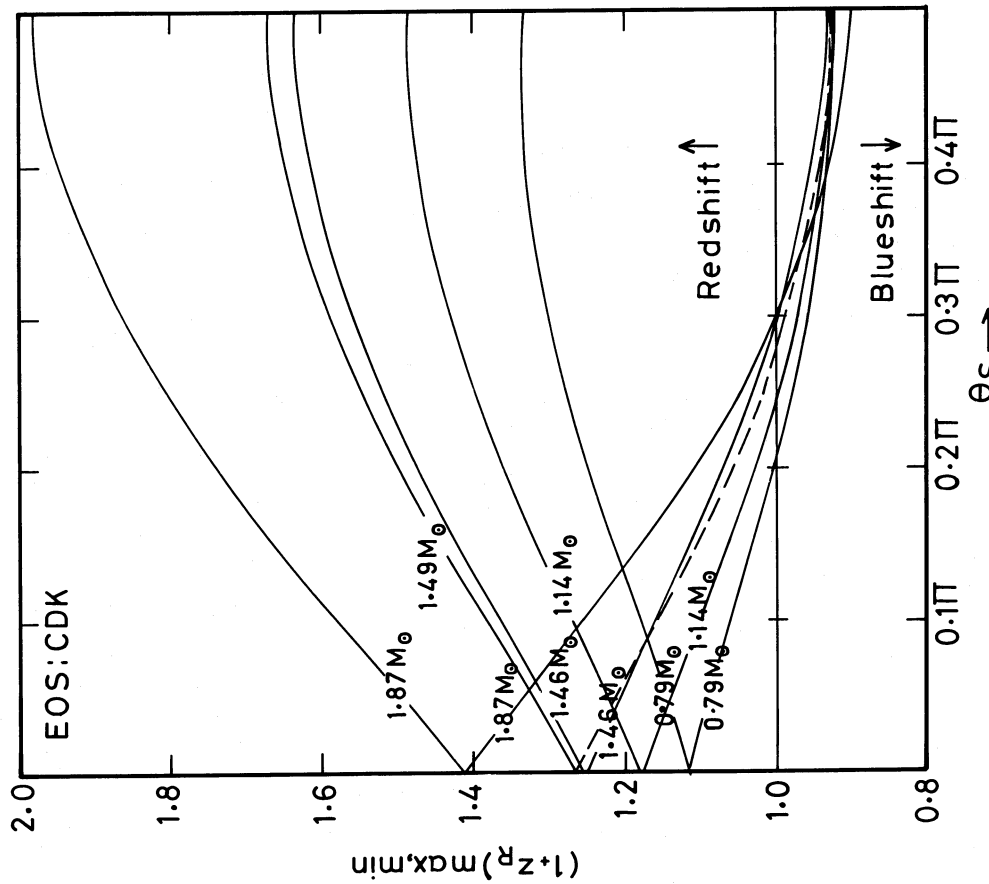

FIG. 5.—Same as Fig. 3, but for EOS model: CDK

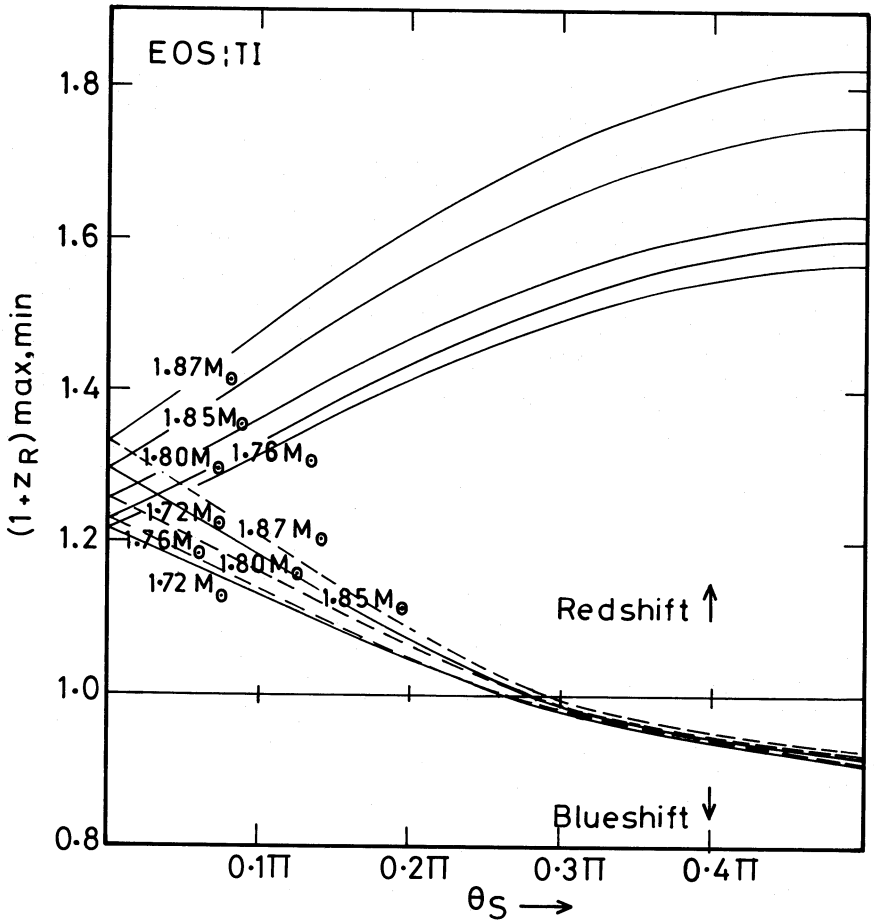

FIG. 7.—Same as Fig. 3, but for EOS model: TI

details of line profile calculation for the moment, the magnitude of the expected asymmetry can be calculated (Kapoor and Datta 1984); the intensity ratio (r_{IN}) at two ends of the broadened spectral line will vary from 1 for $\theta_s = 0$ to a certain maximum value as $\theta_s \to \pi/2$ (Fig. 11). It could be as high as ~ 45 for the 2.085 $M_\odot$ mass FP configuration. We wish to emphasize that the radius of the 2.085 $M_\odot$ mass configuration is $R' = 3.025GM'/c^2$, while the corresponding Schwarzschild configuration has a mass 1.98 $M_\odot$ and a radius $R = 3.168GM/c^2$. It can be shown from a calculation of geodesics in a rotationally perturbed spherical metric that a rotating 2.085 $M_\odot$ mass configuration has its surface within its outer photon sphere, whereas its corresponding Schwarzschild sphere will not be so. Consequently, there will be a trapping of photons by the 2.085 $M_\odot$ FP model rotating configuration. This will limit the angles of emission to $-\delta_2 \leq \delta \leq \delta_1$, where $|\delta_{1,2}|$ are somewhat less than $\pi/2$. Photons emitted outside this "cone" will be gravitationally trapped by the star which, in turn, will get heated up. The line width W and the intensity ratio r_{IN} will then correspond to the above range of δ which can be ascertained from a knowledge of particle orbits in the exterior rotationally perturbed spherical metric. This phenomenon of photon trapping is at present under study. Therefore, in the absence of a quantitative knowledge of δ_1 and δ_2 for the 2.085 $M_\odot$ FP model we have omitted in Figures 4, 10, and 11 curves for Z_R, the line width, and intensity ratio of a gamma-ray line.

A few comments regarding some of the underlying assumptions of our calculations are in order before we proceed to look for the possible astrophysical implications of the results presented here. The first concerns the use of equation (4) to estimate the lower bounds on the redshift parameter. Equation (4) is a particular case ($m = 2$) of secular instability to nonaxisymmetric modes with angular dependence $e^{im\phi}$ (ϕ = azimuthal angle coordinate), and it corresponds to uniform density, uniformly rotating Newtonian configurations such as the Maclaurin sequence (Tassoul 1978). Neutron stars are relativistic configurations. However, because density profiles of neutron stars are believed to be remarkably flat, they may be presumed to resemble the Maclaurin sequence in order to serve as an approximate guide to get an idea of the rotational instabilities. Equation (4) must be viewed as such. Friedman (1983) suggests that the $m = 3$ or $m = 4$ mode is perhaps a more likely candidate to set the limit on rotation in relation to the stability, and the limiting frequency can be in the range $(0.55–0.75)\Omega_c$ instead of equation (4) (see Friedman, Ipser, and Parker 1986). It may be mentioned here that if neutron star interiors possess a large bulk viscosity (which will be the case if, for example, there is a significant concentration of hyperons), then because viscosity is expected to damp out a gravitational wave–driven instability (that arises due to nonaxisymmetric perturbation modes), the above conclusion regarding the $m = 3$ or 4 mode will not be valid. Clearly, there is a need for a fuller and more detailed understanding of the various points of rotational instability for realistic and relativistic neutron star models.

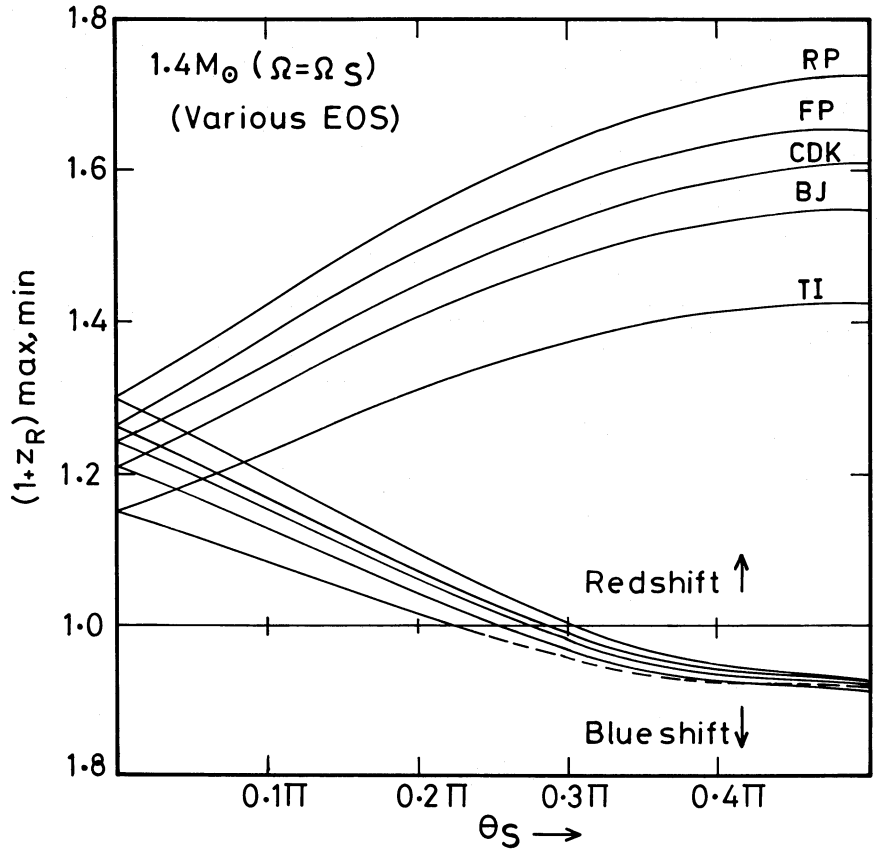

FIG. 8.—Same as Fig. 3, but for a 1.4 $M_{\odot}$ secularly rotating configuration and for various EOS models

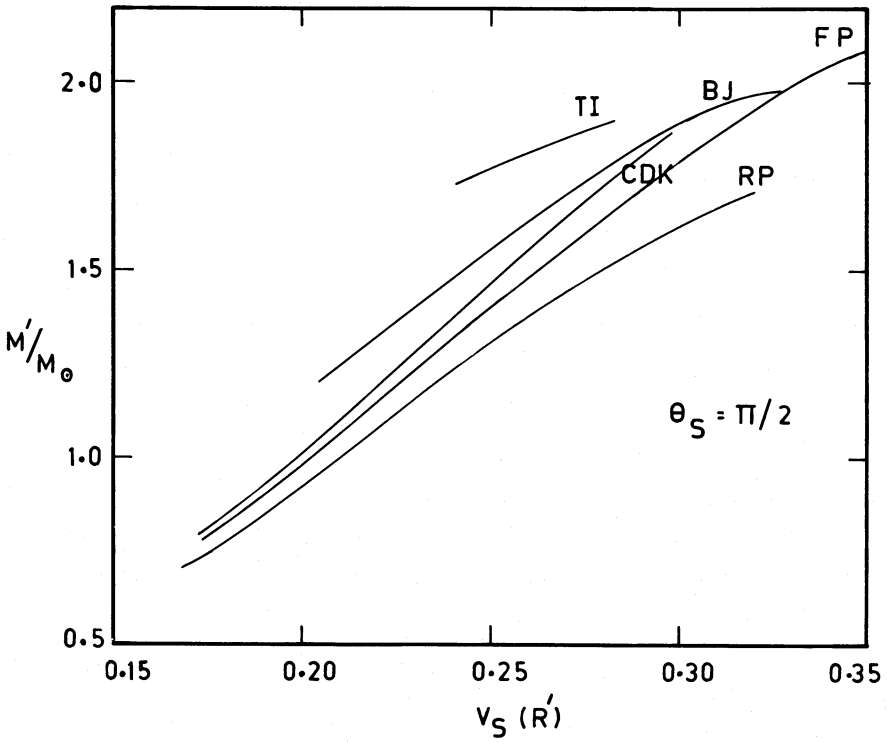

FIG. 9.—Variation of tangential equatorial velocity (V_s) as a function of mass of the secularly rotating neutron star (see text for definition of V_s)

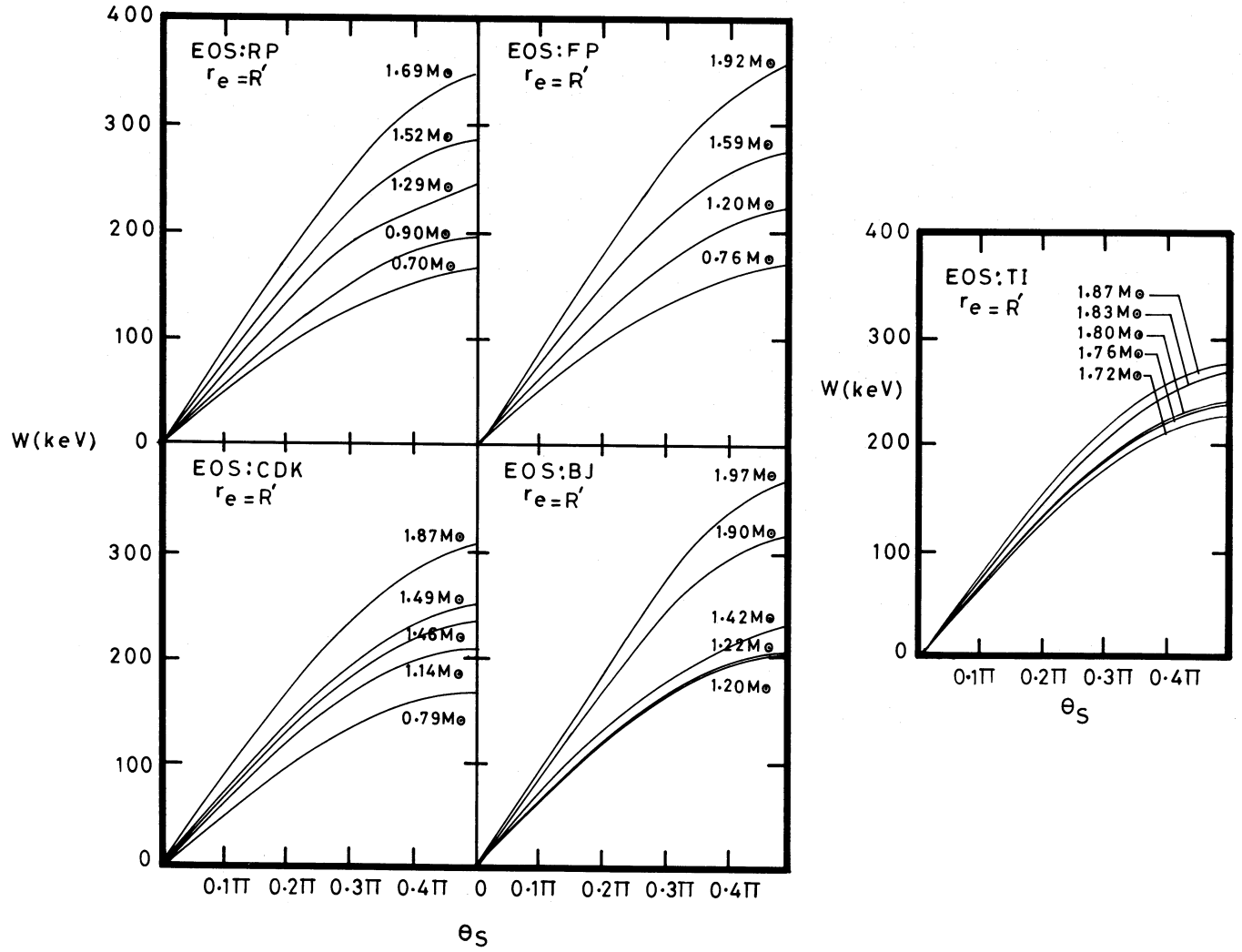

FIG. 10.—Gamma-ray line widths (W) as a function of polar angle of emission θ_s for various EOS models. The mass range is as detailed in Table 1.

Equation (4) provides only a first (semi-Newtonian) estimate of the rotational instability in fast pulsars. Even so, this represented useful information valid for the class of neutron stars associated with fast pulsars, in view of the fact that a satisfactory quantitative estimate of the lightest possible neutron star mass is otherwise not available.

The second comment concerns the use of the Hartle formalism. There is now available a numerical study of rotating neutron stars that incorporates higher order effects of rotation beyond those considered by Hartle (see Friedman, Ipser, and Parker 1986). Insofar as the study of the neutron star redshift is concerned, it is well known that the surface redshift parameter can serve as a guide to estimate the structure of the neutron star and therefore, provides a handle to decide on the equation of state. This important correspondence between the redshift parameter and the equation of state holds good in the case of rapidly rotating neutron stars as well, where there will be additional features like Doppler broadening of surface line emission and steep line profiles caused by rotation (Kapoor and Datta 1984). The dependence on mass (of the rotating neutron stars) of these important rotation induced features is not discernible in the work of Friedman, Ipser, and Parker (1986), where the $R(\theta)$ relationships, the crucial imput for such calculations, are not illustrated. In the absence of such detailed polar angle dependence of the structural parameters, the use of the Hartle prescription constitutes an important first estimate to obtain a trend in relevant astrophysical situations.

To summarize, in this paper we have presented results of a numerical study of the contribution of Doppler effect to frequency shifts in radiation from rapidly rotating neutron stars as a function of their mass. We find a marked competition between rotation and spacetime curvature for forward radiation. Yet the latter dominates over the Doppler effect for the *entire* stable mass range and for a wide range of polar inclination angles.

The results indicate a substantial line broadening and a large asymmetry in the line profile when rotation rates are large (corresponding to millisecond periods). In view of this, the concept of detection of line emission as a line from rapidly rotating neutron stars (and the associated interpretation for the mass-to-radius ratio of the star) will *no longer* hold good. An important conclusion that follows is this: detection of line emission from neutron stars in high-energy radiation sources (such as X-ray or gamma-ray sources) where large rotation rates of the star are otherwise inferred would then imply that the emission region is located far away from the neutron star

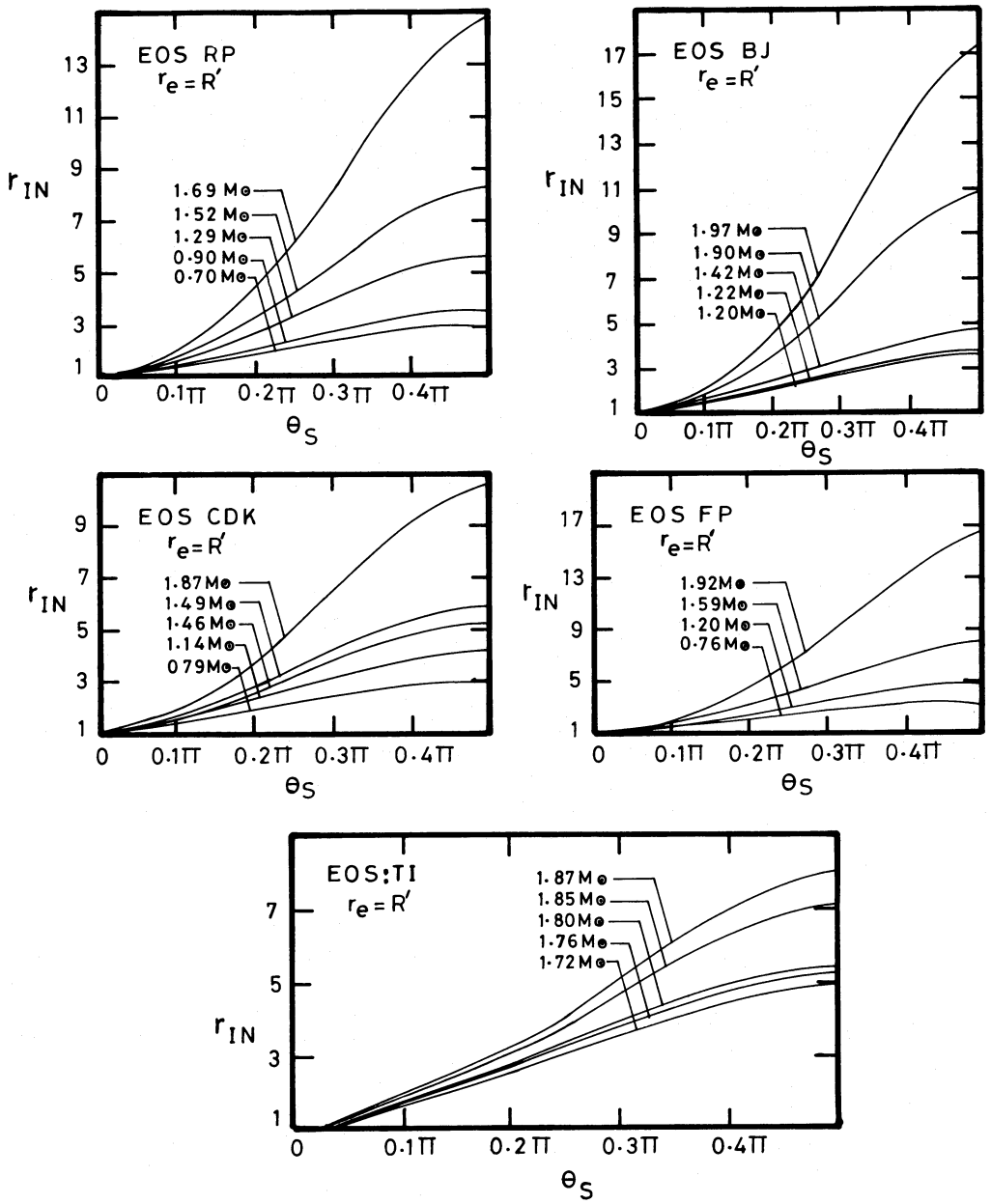

FIG. 11.—Variation of intensity ratio (r_{IN}) as a function of polar angle of emission θ_s for various EOS models. The mass range is as detailed in Table 1.

surface. This in turn would suggest a nonaccretion scenario for the gamma-ray line emission.

B. D. acknowledges Indian National Science Academy for award of a Biren Roy Memorial Trust Fellowship, and R. C. K. thanks Professor Abdus Salam, ICTP, Trieste for hospitality.

REFERENCES

Datta, B., and Kapoor, R. C. 1985, *Nature*, **315**, 557.
Datta, B., and Ray, A. 1983, *M.N.R.A.S.*, **204**, 75p.
Friedman, J. L. 1983, *Phys. Rev. Letters*, **51**, 11.
Friedman, J. L., Ipser, J. R., and Parker, L. 1986, *Ap. J.*, **304**, 115.
Hartle, J. B. 1967, *Ap. J.*, **150**, 1005.
Imamura, J. N., Steiman-Cameron, T. Y., and Middleditch, J. 1987, *Ap. J. (Letters)*, **314**, L11.
Joss, P. C., and Rappaport, S. 1984, *Ann. Rev. Astr. Ap.*, **22**, 537.
Kapoor, R. C., and Datta, B. 1984, *M.N.R.A.S.*, **209**, 895.
———. 1985, *Ap. J.*, **297**, 413.
———. 1986, *Ap. J.*, **311**, 680.
Lindblom, L. 1984, *Ap. J.*, **278**, 364.
Ray, A., and Datta, B. 1984, *Ap. J.*, **282**, 542.
Tassoul, J. L. 1978, *Theory of Rotating Stars* (Princeton: Princeton University Press).

B. DATTA and R. C. KAPOOR: Indian Institute of Astrophysics, Bangalore-560 034, India